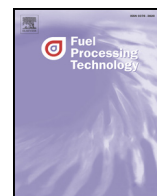




Contents lists available at ScienceDirect

Fuel Processing Technology

journal homepage: www.elsevier.com/locate/fuproc

Research article

Carbon nanofibers and nanospheres-supported bimetallic (Co and Fe) catalysts for the Fischer–Tropsch synthesis

José Antonio Díaz^{a,*}, Amaya Romero^b, Alba María García-Minguillán^a,
Anne Giroir-Fendler^c, Jose Luis Valverde^a

^a Facultad de Ciencias y Tecnologías Químicas, Departamento de Ingeniería Química, Universidad de Castilla la Mancha, Avenida de Camilo José Cela 12, 13071 Ciudad Real, Spain

^b Escuela de Ingenieros Agrónomos, Departamento de Ingeniería Química, Universidad de Castilla la Mancha, Avenida de Camilo José Cela 12, 13071 Ciudad Real, Spain

^c Université Claude Bernard Lyon 1, Villeurbanne, F-69622, CNRS, UMR 5256, IRCELYON, 2 Avenue Albert Einstein, Villeurbanne, F-69622, France

ARTICLE INFO

Article history:

Received 24 February 2015

Received in revised form 5 June 2015

Accepted 7 June 2015

Available online xxx

Keywords:

Fischer–Tropsch

Carbon nanofibers

Carbon nanospheres

Cobalt

Iron

ABSTRACT

The present work compares the physicochemical properties of carbon nanofibers (CNF) and carbon nanospheres (CNS)-supported bimetallic cobalt and iron catalysts and their performance in the Fischer–Tropsch synthesis (FTS), at 523 K and 20 bar. Supports were characterized by N₂ adsorption–desorption, temperature-programmed reduction (TPR) and decomposition under He atmosphere (TPD-He), X-ray diffraction (XRD) and Raman spectroscopy. Catalysts were in turn characterized by inductively coupled plasma spectrometry (ICP), N₂ adsorption–desorption, TPR, XRD and transmission electron microscopy (TEM). Results showed that the bimetallic catalyst supported over CNF was highly active in the conversion of CO and H₂ to hydrocarbons and selective towards gasoline and kerosene fractions. On the other hand, catalyst supported over CNS presented small and well-dispersed metal particles which strongly interacted with the support and, as a consequence, promoted the reactants conversion in a lesser extent and favoured the growth of hydrocarbon chains.

© 2015 Elsevier B.V. All rights reserved.

1. Introduction

Carbonaceous supports are widely used in heterogeneous catalysis due to their resistance to acidic/basic media, adjustable porosity by changing the synthesis reaction conditions, surface chemistry and easy recovery of the supported metal by controlled combustion [1]. Over the last years, some new carbon nanostructures with different properties have been discovered. Therefore, the deposition of the active phase and the further catalytic activity will depend on the chosen nanostructure.

Carbon nanofibers (CNF) are cylindrical or conical structures that have diameters varying from a few to hundreds of nanometres and lengths from lesser than a micron to millimetres. The internal structure of CNF consists of different arrangements of graphene layers [2]. These layers present some defects, which lead to the occurrence of mesopores that confers a medium specific surface area (10–200 m²·g⁻¹). The mesoporous character weakens the mass transfer constraints. Carbon nanospheres (CNS) are presented as a conglomeration of spherical bodies with low specific surface areas (<20 m²·g⁻¹). CNS have a high surface chemical activity provided by “unclosed” graphitic layers, reactive open edges and “dangling bonds” that can enhance reactant adsorption. Different CNS synthesis methods have been proposed in the

literature, which provided spheres with a wide variety of diameters and crystalline nature [3]. In this regard, Serp et al. [4] classified CNS in three categories by considering the size of these structures: well-graphitised onion like structures (diameters 2–20 nm), less graphitised carbon spheres (diameters 50 nm–1 μm) and carbon beads (diameters 1–several μm).

CNF have been proven to be an efficient catalyst support in many reactions of industrial interest [5–7]. On the other hand, CNS have been discovered recently, so that there are only a few works that deal with the use of CNS as a catalyst support [8–10]. However, their properties abovementioned make them a promising support of catalysts for industrial applications like the Fischer–Tropsch synthesis.

Fischer–Tropsch synthesis (FTS) is a heterogeneously catalyzed polymerization process that converts syngas (CO and H₂) into a wide variety of hydrocarbons, which constitutes a promising route for the production of clean liquid fuels. The product distribution in the FTS is very broad. Consequently, many studies have been carried out with the aim of controlling and limiting the product selectivity. Ruthenium-, iron- and cobalt-based catalysts have been used in this process, but the latter (Co- and Fe-based catalysts) are the most widely studied since, despite that Ru shows good catalytic properties, its annual world supply cannot even fulfil the requirements of an average plant [11]. Under the same experimental conditions, Fe-based catalysts lead to the formation of light hydrocarbons and small amounts of CH₄ in comparison to Co-based ones. On the other hand, Co-based catalysts show high catalytic activity and are

* Corresponding author.

E-mail address: joseantonio.diaz@uclm.es (J.A. Díaz).

suitable for the production of middle distillates and waxes, but they are more expensive.

In recent years, the preparation of bimetallic Co:Fe catalysts to be used in FTS has gained a growing interest. It has been reported that the simultaneous use of Fe and Co gives rise to a synergistic effect between the two active phases [12–14]. Co:Fe metal mixtures have been traditionally supported on typical FTS supports such as silica [13,15,16], titania [17,18] and alumina [14]. However, several studies related to the preparation of bimetallic catalysts supported on carbonaceous materials and their use in FTS can be found in the literature [19].

In this work, Co:Fe bimetallic catalysts supported on CNF and CNS were prepared. The different properties of CNF and CNS were evaluated, as well as the influence of these properties over the active phase deposition, and therefore the catalytic activity of the resulting catalysts in the FTS. According to a previous work of our group [20], an optimal metal content of ca. 10 wt.% of Co and 5 wt.% of Fe was set for both catalysts.

2. Experimental

CNF were prepared, according to the procedure described elsewhere [21] by the catalytic decomposition of ethylene over a Ni/SiO₂ catalyst at 873 K. On the other hand, CNS were prepared by the pyrolysis of benzene at 1223 K [22]. Bimetallic Co:Fe catalysts were prepared by the incipient wetness impregnation method using aqueous solutions of Co(NO₃)₂·6H₂O and Fe(NO₃)₃·9H₂O (MERCK), respectively. The catalyst support was placed in a glass vessel and kept under vacuum at room temperature for 2 h to remove water and other impurities adsorbed on the structure. A known volume of two aqueous solutions (the minimum amount required to wet the solid) was then poured simultaneously over the support. The solvent was then removed by evaporation under vacuum at 363 K for 2 h. The final catalysts were dried at 403 K overnight and sieved into a batch with an average diameter of 254 μm.

Cobalt and/or iron content were measured by using an inductively coupled plasma spectrometer (ICP, Model Liberty Sequential, Varian). Samples were diluted to 50:50 (v/v) by using a 4 N nitric acid solution, in order to ensure the total solubility of the metal. Surface area/porosity measurements were conducted using a Quantachrome Quadrasorb SI apparatus with N₂ as the sorbate at 77 K. All samples were outgassed prior to analysis at 453 K under vacuum (1 × 10⁻² Torr) for 12 h. The total specific surface area and mesoporosity were determined by the multipoint BET and the Barret–Joyner–Halenda (BJH) methods, respectively. XRD analyses were conducted with a Philips X'Pert instrument using nickel-filtered Cu-Kα radiation. Samples were scanned at a rate of 0.02°·step⁻¹ over the range 5° ≤ 2θ ≤ 90° (scan time = 2 s·step⁻¹), and the diffractograms were compared with those of the PDF-ICDD references. Interlayer spacing (d₀₀₂) was determined from the (002) diffraction peak position (Bragg equation) and the stacking height of the crystallites (L_c) was determined using the Scherrer equation. Micro-Raman spectrum of the supports were recorded with a Renishaw Raman Microscope System RM1000 equipped with a Leica microscope, an electrically refrigerated CCD camera and a diode laser at 514 nm as the excitation source, operating at a power level of 3 mW. The planar crystallite size (L_a) for the samples was calculated from the intensities of D and G bands on the RAMAN spectra using Tuinstra and Koenig (T–K) relation (L_a (nm) = 4.4 / (I_D / I_G)) [23]. Temperature-programmed reduction (TPR) and decomposition under helium atmosphere (TPD–He) experiments were conducted in a commercial Micromeritics AutoChem 2950 HP unit with TCD detection. On the one hand, TPR samples (ca. 0.15 g) were loaded in a U-shaped quartz reactor and ramped from room temperature to 1173 K (5 K·min⁻¹) under a reducing atmosphere (17.5% v/v H₂/Ar, 60 cm³·min⁻¹). On the other hand, TPD–He samples (ca. 0.1 g) were loaded in the same reactor and ramped to 1173 K (5 K·min⁻¹) in a flow of He (100 cm³·min⁻¹). Transmission electron microscopy (TEM) analysis performed employed a JEOL JEM-4000EX unit with an accelerating voltage of 400 kV. Samples were

prepared by ultrasonic dispersion in acetone with a drop of the resultant suspension evaporated onto a holey carbon-supported grid. Mean metal particle size evaluated as the surface-area weighted diameter (\bar{d}_s) was computed according to (Eq. (1)):

$$\bar{d}_s = \frac{\sum_i n_i d_i^3}{\sum_i n_i d_i^2} \quad (1)$$

where n_i represents the number of particles with diameter d_i ($\sum_i n_i \geq 200$). The standard deviation (σ) of the obtained \bar{d}_s was calculated with the following formula (Eq. (2)):

$$\sigma = \sqrt{\frac{\sum_{i=1}^n (x_i - \bar{x})^2}{n}} \quad (2)$$

FTS catalytic activity was tested in a stainless steel fixed bed reactor (9 mm i.d. × 305 mm length) provided with a porous plate (2 μm pore size). Initially, the catalyst bed (2 g) was activated at 623 K (heating ramp of 5 K·min⁻¹) for 5 h with a flow rate of 100 N ml·min⁻¹ of ultrapure hydrogen. The reactor was then cooled and pressurized up to reaction conditions (523 K and 20 bar, respectively) under a N₂ atmosphere (100 N ml·min⁻¹). A flow of a mixture of CO, H₂ and N₂ (CO:H₂:N₂ volume ratio of 3:6:1, N₂ used as the internal standard) was established through the reactor during 48 h, with a constant gas hourly space velocity (GHSV) of 3000 N ml·g⁻¹·h⁻¹. The product stream was cooled in a Peltier cell (T ≈ 278 K) and collected for analysis. Liquid samples (C₇–C₂₀) were analysed off-line by capillary GC (VARIAN 430) equipped with a flame ionization detector (FID). C₁–C₆ hydrocarbons, unreacted CO and H₂, N₂ and CO₂ were analysed on-line by GC (VARIAN 4900). Calibrations were performed with standard samples for data quantification. The CO reaction rate was determined by using the following equation:

$$rate = \frac{N_{CO,converted}(\text{mol}/\text{min})}{(m_{cobalt+iron})(\text{mol})} \quad (3)$$

Selectivity to gaseous products (CO₂, CH₄, C₂H₆ and C₃H₈) was obtained by using Eq. (4), whereas that of long-chain hydrocarbons (C₅₊) was estimated by using Eq. (5):

$$S_p(\%) = \frac{N_p(\text{mol}/\text{min})}{N_{CO,feed}(\text{mol}/\text{min})} \cdot 100 \quad (4)$$

$$S_{C_{5+}}(\%) = 100 - \sum_p S_p \quad (5)$$

Finally, the yield of long-chain hydrocarbons (C₅₊) was calculated using the following equation:

$$yield_{C_{5+}} = \frac{N_{CO,converted}(\text{mol}/\text{min})}{N_{CO,feed}(\text{mol}/\text{min})} \cdot S_{C_{5+}} \quad (6)$$

3. Results and discussion

3.1. Supports and catalyst characterization

The physicochemical properties and nitrogen adsorption–desorption isotherms of both the supports and the prepared catalysts are shown in Table 1 and Fig. 1, respectively.

The support CNF and the catalyst CoFe/CNF showed isotherms corresponding to a type IV according to the IUPAC classification, which are characteristic of mesoporous materials. These isotherms presented a significant volume increase in the middle relative pressure range (0.3 ≤ P/P₀ ≤ 0.8). The observed H3 hysteresis loops (IUPAC classification)

Download English Version:

<https://daneshyari.com/en/article/6656881>

Download Persian Version:

<https://daneshyari.com/article/6656881>

[Daneshyari.com](https://daneshyari.com)